*J. Fluid Mech.* (1977), *vol.* 81, *part* 1, *pp.* 107–127
*Printed in Great Britain*



# Instabilities of longitudinal convection rolls in an inclined layer

By R. M. CLEVER

Mechanics and Structures Department, University of California, Los Angeles

AND F. H. BUSSE

Institute of Geophysics and Planetary Physics, University of California, Los Angeles

(Received 12 August 1975 and in revised form 8 September 1976)

The stability of longitudinal rolls in an inclined convection layer is investigated for various angles of inclination. Three types of instability are responsible for the transition from longitudinal rolls to three-dimensional forms of convection in different regimes of the parameter space. The role of the wavy instability is emphasized since it does not correspond to a transition in the case of a horizontal layer. The analysis emphasizes the cases of air and water as convective media. Comparison of the theoretical results with experimental data indicates that the stability analysis based on infinitesimal disturbances correctly describes the observed instabilities.

## 1. Introduction

In recent years convection in a fluid layer heated from below has received considerable attention as a hydrodynamic system which exhibits the phenomenon of turbulence with particular simplicity. Because of the relative ease with which the onset of convection and higher transitions can be observed experimentally as well as investigated theoretically convection has become a prime example for the understanding of the transition to turbulence in fluid systems.

Most of the attention has been focused on the case of a horizontal convection layer, which has the property that the physical conditions in the horizontal direction are isotropic and homogeneous at least in the theoretical idealization of a layer of infinite extent. The onset of convection in this case is determined by a single parameter, the Rayleigh number, which describes the ratio between the energy released by the buoyancy force and the energy dissipated by viscous friction and thermal conduction. Even though the mechanism of the release of thermal energy driving convection is basically simple, a rich variety of phenomena is displayed by finite amplitude convective motions. This variety stems primarily from the dependence of the motions on the Prandtl number, which represents the second non-dimensional parameter of the problem. At high Prandtl numbers the nonlinear terms in the equation of motion are of minor importance and the properties of convection are dominated by the thermal boundary layers. The instability of the thermal boundary layers causes a transition to bimodal convection, which is well understood from both the theoretical (Busse 1967*a*) and the experimental (Krishnamurti 1970*a*; Busse & Whitehead 1971) points

of view. At Prandtl numbers of order unity and lower the momentum terms cause a transition from convection rolls to time-dependent oscillatory convection. While the Rayleigh number for the transition to bimodal convection depends only slightly on the Prandtl number, a strong dependence is exhibited by the Rayleigh number at which the onset of oscillations occurs. Experimental observations of the oscillatory instability (Willis & Deardorff 1970; Krishnamurti 1970*b*, 1974) have preceded the theoretical investigations (Busse 1972; Clever & Busse 1974), which are complicated by the property that vertical vorticity associated with the oscillations enters the problem as an additional variable. Other instabilities, such as the zigzag instability, have been predicted (Busse 1967*a*) and observed (Busse & Whitehead 1971) in the case where the convection-roll wavelength differs sufficiently from its optimal value. In the case of a horizontal layer the zigzag instability, as well as the Eckhaus instability (Busse 1971), does not correspond to a transition to a new form of convection.

In this paper we intend to extend the picture described above to the case of convection in an inclined layer. This case differs considerably from the horizontal case because of the direction distinguished by the downslope component of gravity. The characteristic degeneracy of the eigenvalue problem for the onset of convection in a horizontal layer is removed and a single form of convection is realized. Except in the case of low Prandtl number or nearly vertical inclination of the layer, when a transverse mode is preferred, convection assumes the form of longitudinal rolls aligned with the direction of inclination. The uniqueness of the two-dimensional convection solution at the critical Rayleigh number contrasts with the random orientation of convection rolls found in a horizontal layer. The randomness represents a typical property of turbulence in a case when motions are still steady. From this point of view the transition to a three-dimensional form of convection in the inclined layer is an even more important step in the development towards turbulence than in the horizontal layer. We shall consider this problem by analysing the dependence of the various instabilities of the longitudinal convection rolls on both the Prandtl number and the angle of inclination.

The interest in a non-isotropic case of convection in contrast to the horizontally isotropic convection layer is not the only motivation for the present analysis. An inclined layer with different temperatures prescribed on the boundaries exhibits a plane parallel shear flow in the absence of convection. The interaction of convection and shear flow, however, is an important phenomenon in meteorological and other geophysical applications. Convection in the presence of a mean shear is not easily realized in the laboratory. For this reason the case of an inclined convection layer has received particular attention from experimentalists, even though the problem differs in some respects from the case of a horizontal layer with superimposed shear. The availability of detailed data (especially those obtained by Hart 1971*a*, *b*) on higher transitions of convection flows in an inclined layer has provided the challenge for the work described in this paper. Another case of convection in the presence of shear flow is provided by the thermal boundary layer on an inclined heated plate in an infinite fluid. Experimental realizations of this case (Sparrow & Husar 1969) show phenomena similar to those observed by Hart.

The linear stability analysis of an unstably stratified layer with a mean shear flow shows that either longitudinal or transverse rolls or travelling waves set in depending on the magnitude of the shear and the Prandtl number. While the shear flow does not

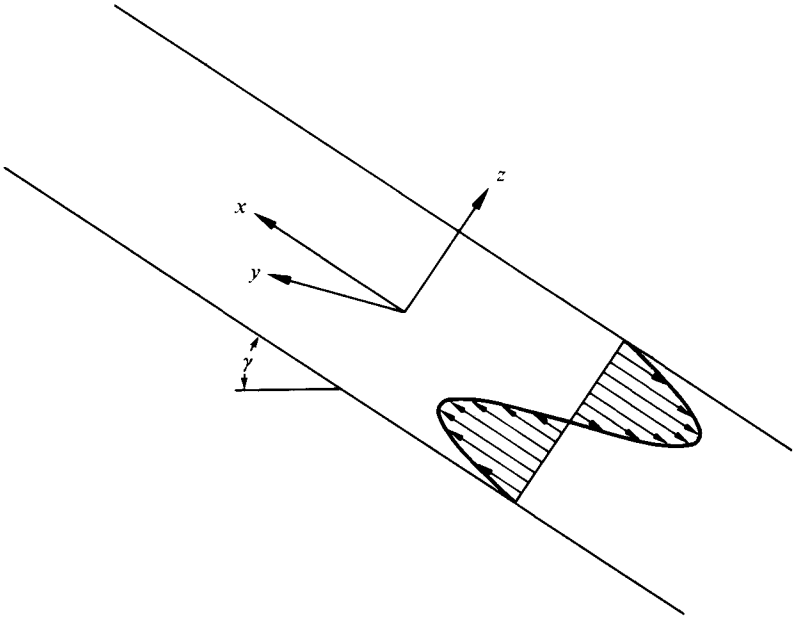


FIGURE 1. Co-ordinate system for the inclined layer.

influence the onset of longitudinal rolls it may have a destabilizing or a stabilizing effect on the onset of the transverse mode. Although the present paper investigates only the finite amplitude properties and stability characteristics of the longitudinal convection rolls, we expect that the destabilizing influence of the shear flow will become noticeable for certain parts of the parameter range and that the transverse mode will reappear in the form of an instability. This aspect of the problem of the interaction of convection with shear will be discussed in detail in § 7.

The paper starts with the formulation of the basic equations of the problem in § 2. In § 3 the steady solution in the form of finite amplitude longitudinal convection rolls is discussed. The solution is identical to the corresponding solution in a plane layer except for an additional component of the velocity field in the direction of the mean flow, which can be calculated separately, as was shown by Clever (1973). In § 4 the stability analysis is formulated. The wavy instability (standing waves) which predominates in experimental studies is investigated in § 5. A competitor of the wavy instability at low angles of inclination is the oscillatory instability (travelling waves), which is discussed in § 6. Finally, the problem of the transverse instability is analysed in § 7.

## 2. Basic equations

We consider a fluid layer of infinite extent inclined at an angle $\gamma$ with respect to the horizontal. Constant temperatures $T_1$ and $T_2$ ($T_2 > T_1$) are prescribed at the upper and lower boundaries of the layer. For the non-dimensional description of the problem we shall use the thickness $d$ of the layer as the length scale, $d^2/\kappa$, with $\kappa$ denoting the thermal diffusivity, as the time scale and $(T_2 - T_1)/R$ as the temperature scale. Accord-

ingly, the Navier–Stokes equations for the velocity vector $\mathbf{u}$ and the heat equation for the temperature $\Theta$ are

$$\nabla^2\mathbf{u} + \Theta(\mathbf{k} + \mathbf{i}\tan\gamma) - \nabla\pi = P^{-1}(\partial\mathbf{u}/\partial t + \mathbf{u}.\nabla\mathbf{u}), \tag{2.1a}$$

$$\nabla.\mathbf{u} = 0, \tag{2.1b}$$

$$\nabla^2\Theta + R\mathbf{k}.\mathbf{u} = \partial\Theta/\partial t + \mathbf{u}.\nabla\mathbf{u}. \tag{2.1c}$$

The unit vector $\mathbf{k}$ is normal to the layer and the unit vector $\mathbf{i}$ is parallel to it and in the direction of inclination, as shown in figure 1. The physical properties of the system are described by two non-dimensional parameters, namely the Rayleigh number $R$ and the Prandtl number $P$:

$$R \equiv \beta g \cos\gamma (T_2 - T_1) d^3/\nu\kappa, \quad P \equiv \nu/\kappa, \tag{2.2}$$

where $\nu$ is the kinematic viscosity, $g$ the acceleration due to gravity and $\beta$ the coefficient of expansion. We have assumed the Boussinesq approximation, in which the density is regarded as a constant except in the gravity term. All terms which can be expressed as gradients are combined in the 'pressure' gradient term $\nabla\pi$.

The basic solution of (2.1) consists of a temperature distribution governed by conduction only and a plane parallel flow in the direction of inclination. Using a Cartesian system of co-ordinates with the origin at the centre of the layer and the $x$ and $z$ co-ordinates in the directions of $\mathbf{i}$ and $\mathbf{k}$, we find the basic solution

$$\Theta_0 = -Rz + \frac{T_1 + T_2}{2(T_2 - T_1)} R, \tag{2.3a}$$

$$\mathbf{U}_0 = \mathbf{i}R\tan\gamma \times \tfrac{1}{6}(z^3 - \tfrac{1}{4}z) \equiv U_0\mathbf{i}. \tag{2.3b}$$

In deriving this solution we have used the condition that the velocity vector vanishes at the rigid boundaries. In order to describe the secondary solution corresponding to the convective state of the system we write

$$\mathbf{u} = \mathbf{U} + \mathbf{v} = \mathbf{U}_0 + \mathbf{U}_1 + \mathbf{v}, \quad \Theta = \Theta_0 + \theta,$$

where $\mathbf{U}_1$ denotes the purely $z$-dependent modification of the basic mean flow profile (2.3$b$) owing to the onset of convection. The fluctuating component $\mathbf{v}$ of the velocity field is defined by the property that its $x$, $y$ average, indicated by an overbar, vanishes:

$$\bar{\mathbf{v}} = \bar{\mathbf{u}} - \mathbf{U} = 0.$$

It is convenient to eliminate the equation of continuity (2.1$b$) by introducing the general representation for the solenoidal vector field $\mathbf{v}$:

$$\mathbf{v} = \boldsymbol{\delta}\phi + \boldsymbol{\epsilon}\psi, \tag{2.4}$$

where $$\boldsymbol{\delta}\phi \equiv \nabla \times (\nabla \times \mathbf{k}\phi), \quad \boldsymbol{\epsilon}\psi = \nabla \times \mathbf{k}\psi.$$

After operating with $\mathbf{k}.\nabla\times(\nabla\times\ldots)$ and $\mathbf{k}.\nabla\times$ on (2.1$a$) and subtracting the equation satisfied by $\Theta_0$ from (2.1$c$) we obtain the following equations for the scalar variables $\phi$, $\psi$ and $\theta$:

$$\begin{aligned}\nabla^4\Delta_2\phi + \tan\gamma\,\partial^2_{xz}\theta - \Delta_2\theta = P^{-1}\{&\boldsymbol{\delta}.[(\boldsymbol{\delta}\phi + \boldsymbol{\epsilon}\psi).\nabla(\boldsymbol{\delta}\phi + \boldsymbol{\epsilon}\psi)] \\ &+ (U\partial_x + \partial_t)\nabla^2\Delta_2\phi - \partial^2_{zz}U\partial_x\Delta_2\phi\},\end{aligned} \tag{2.5a}$$

$$\nabla^2\Delta_2\psi + \tan\gamma\,\partial_y\theta = P^{-1}\{\epsilon_0[(\delta\phi+\epsilon\psi).\nabla(\delta\phi+\epsilon\psi)] + (U\partial_x+\partial_t)\Delta_2\psi - \partial_z U\partial_y\Delta_2\phi\}, \tag{2.5b}$$

$$\nabla^2\theta - R\Delta_2\phi = (\delta\phi+\epsilon\psi).\nabla\theta + (U\partial_x+\partial_t)\theta. \tag{2.5c}$$

Anticipating that $\mathbf{U}_1$ is directed solely in the $x$ direction because of the symmetry of the problem we have used $\mathbf{U} = \mathbf{i}U$. The symbol $\Delta_2$ denotes the Laplacian with respect to the $x, y$ plane, i.e.

$$\Delta_2 \equiv \partial^2_{xx} + \partial^2_{yy}.$$

The boundary conditions for $\phi$, $\psi$ and $\theta$ are

$$\phi = \partial_z\phi = \psi = \theta = 0 \quad \text{at} \quad z = \pm\tfrac{1}{2}. \tag{2.6}$$

The goal of the following analysis is first to obtain steady solutions of (2.5) and then to investigate the stability properties of the steady solutions. In experiments two different kinds of steady solution of (2.5) are observed: longitudinal rolls, which are independent of the $x$ co-ordinate, and transverse rolls, which do not exhibit a $y$ dependence. In both cases (2.5*a*, *c*) can be solved independently of (2.5*b*). For transverse rolls $\psi$ vanishes. For longitudinal rolls a non-vanishing $\psi$ is obtained from (2.5*b*). In fact, it is because of the additional velocity component in the $x$ direction that the longitudinal-roll solution differs from the corresponding solution in a horizontal layer. We shall discuss this point in more detail in the following section. The transverse-roll solution will not be considered in this paper since it occurs only for large values of the parameter $P^{-1}\tan\gamma$, or for angles of inclination at which the heating is from above.

## 3. Longitudinal convection rolls

For steady longitudinal rolls the $x$ and $t$ dependence vanishes and (2.5) can be simplified considerably to (see also Hart 1973)

$$\partial_y(\nabla^4\phi - \theta) = P^{-1}\{\partial^2_{yz}\phi\partial^2_{yy}\nabla^2\phi - \partial^2_{yy}\phi\partial^2_{yz}\nabla^2\phi\}, \tag{3.1a}$$

$$\partial_y(\nabla^2\partial_y\psi + \tan\gamma\theta) = P^{-1}\partial_y\{\partial^2_{yz}\phi\partial^2_{yy}\psi - \partial^2_{yy}\phi\partial_{yz}\psi - \partial_z U\partial^2_{yy}\phi\}, \tag{3.1b}$$

$$\nabla^2\theta - R\partial^2_{yy}\phi = \partial^2_{yz}\phi\partial_y\theta - \partial^2_{yy}\phi\partial_z\theta. \tag{3.1c}$$

In order to solve these equations the function $U$ must be determined. While $U_0$ is given by (2.3*b*), $U_1$ is obtained from the $y$ average of (2.1*a*):

$$U_1 = -\tan\gamma\int_{-\frac{1}{2}}^{z}\left[\int_{-\frac{1}{2}}^{z'}\overline{\theta}\,dz''\right]dz' + \frac{1}{P}\left[\int_{-\frac{1}{2}}^{z}\overline{\partial^2_{yy}\phi\partial_y\psi}\,dz' + (z+\tfrac{1}{2})\langle\partial_{yy}\phi\partial_y\psi\rangle\right], \tag{3.1d}$$

where the angular brackets denote the average over the entire fluid layer.

It is obvious from (3.1*a*, *b*) that $\phi$ and $\theta$ can be determined independently of $\psi$. Since $\gamma$ does not appear in the problem posed by (3.1*a*, *c*) and the boundary conditions (2.6), the solution for $\phi$ and $\theta$ is identical to the solution for convection rolls in a horizontal layer. Hence the analysis of convection rolls described in Clever & Busse (1974, henceforth referred to as I) can be applied to the present problem. For the problem of the stability of this solution the presence of a normal component of vorticity $\psi$ causes a considerable difference. This will become apparent in a later section of this

paper. The equivalence of longitudinal rolls in an inclined layer and rolls in a horizontal layer has not always been appreciated in the literature. We refer to the discussion by Clever (1973).

Even after (2.3*b*) and (3.1*d*) have been inserted for $U$, (3.1*b*) remains a linear inhomogeneous equation for $\psi$ with the special property that both inhomogeneous terms are proportional to $\tan\gamma$. Hence we need to obtain a solution $\psi_0$ for only one particular angle. For convenience we choose the case $\gamma = \frac{1}{4}\pi$. The general solution for arbitrary angles is then

$$\psi = \psi_0 \tan\gamma. \tag{3.2}$$

In order to solve (3.1*b*) numerically we follow the analysis in I. We expand $\psi_0$ in terms of a double series

$$\psi_0 = \sum_{\lambda,\nu} c_{\lambda\nu} e^{i\lambda\alpha y} f_\nu(z) \equiv \sum_{\lambda,\nu} c_{\lambda\nu} \psi_{\lambda\nu}, \tag{3.3}$$

where the ranges of the summations over $\lambda$ and $\nu$ are $-\infty \leqslant \lambda \leqslant +\infty$ and $1 \leqslant \nu \leqslant \infty$. Here the functions

$$f_\nu(z) \equiv \sin\nu\pi(z+\tfrac{1}{2}) \tag{3.4}$$

satisfy the boundary conditions (2.6) for $\psi$. Since the solution $(\phi, \theta)$ derived in I is symmetric in $y$, $\psi$ must be antisymmetric, i.e.

$$c_{\lambda\nu} = -c_{-\lambda\nu}. \tag{3.5}$$

In addition, we can restrict our attention to coefficients $c_{\lambda\nu}$ with $\lambda+\nu$ even since $\phi$ and $\theta$ have the same symmetry and since $U$ is antisymmetric in $z$. For numerical purposes the infinite series (3.3) must be approximated by a truncated series. Following the procedure in I the truncated series is obtained by neglecting all modes with

$$|\lambda| + \nu > N. \tag{3.6}$$

The same value of $N$ will be used as for the solution for $\phi$ and $\theta$ obtained in I.

By multiplying (3.1*b*) by $\sin\kappa\pi(z+\frac{1}{2})\, f_\mu(z)$ and averaging over the fluid layer we obtain the following set of linear equations for the coefficients $c_{\lambda\nu}$:

$$I^{(7)}_{\kappa\mu\lambda\nu} c_{\lambda\nu} + I^{(8)}_{\kappa\mu\rho\pi} b_{\rho\pi} + P^{-1} I^{(9)}_{\kappa\mu\lambda\nu\rho\pi} a_{\rho\pi} c_{\lambda\nu} + RP^{-1} I^{(10)}_{\kappa\mu\lambda\nu} a_{\lambda\nu} = 0, \tag{3.7}$$

where the summation convention has been assumed.

In addition to (3.3) we have substituted into (3.1*b*) the expansions

$$\begin{aligned} \phi &= \sum_{\lambda,\nu} a_{\lambda\nu} e^{i\lambda\alpha y} g_\nu(z) \equiv \sum_{\lambda,\nu} a_{\lambda\nu} \phi_{\lambda\nu}, \\ \theta &= \sum_{\lambda,\nu} b_{\lambda\nu} e^{i\lambda\alpha y} f_\nu(z) \equiv \sum_{\lambda,\nu} b_{\lambda\nu} \theta_{\lambda\nu} \end{aligned} \tag{3.8}$$

which were introduced in I. The functions $g_\nu(z)$ satisfy the boundary conditions for $\phi$ and are defined by

$$g_\nu(z) = \begin{cases} \dfrac{\sinh(\beta_{\nu/2} z)}{\sinh(\frac{1}{2}\beta_{\nu/2})} - \dfrac{\sin\beta_{\nu/2} z}{\sin(\frac{1}{2}\beta_{\nu/2})} & \text{for } \nu \text{ even}, \\ \dfrac{\cosh(\lambda_{(\nu+1)/2} z)}{\cosh(\frac{1}{2}\lambda_{(\nu+1)/2})} - \dfrac{\cos(\lambda_{(\nu+1)/2} z)}{\cos(\frac{1}{2}\lambda_{(\nu+1)/2})} & \text{for } \nu \text{ odd}, \end{cases} \tag{3.9}$$

where the values of $\beta_\nu$ and $\lambda_\nu$ are the positive roots of

$$\coth\tfrac{1}{2}\beta - \cot\tfrac{1}{2}\beta = 0 \tag{3.10a}$$

and

$$\tanh\tfrac{1}{2}\lambda + \tan\tfrac{1}{2}\lambda = 0. \tag{3.10b}$$

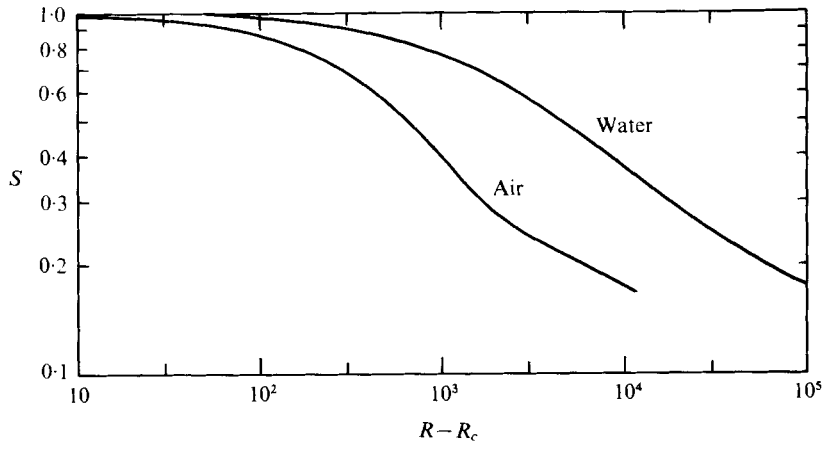


FIGURE 2. The horizontally averaged wall shear stress $S = \partial_z U(z = \frac{1}{2})/\partial_z U_0(z = \frac{1}{2})$.

Chandrasekhar introduced the functions (3.9) into the analysis of convection problems and has computed the roots of (3.10) (Chandrasekhar 1961, p. 635).

We have used superscripts starting with 7 for the matrices in (3.7) in continuation of the analogous analysis in I. The matrices $\mathbf{I}^{(n)}$ with $n \geqslant 7$ are defined by

$$I^{(7)}_{\kappa\mu\lambda\nu} \equiv \langle \psi_{\kappa\mu} \nabla^2 \partial^2_{yy} \psi_{\lambda\nu} \rangle, \quad I^{(8)}_{\kappa\mu\lambda\nu} \equiv \langle \psi_{\kappa\mu} \partial_y \theta_{\lambda\nu} \rangle,$$

$$I^{(9)}_{\kappa\mu\lambda\nu\rho\pi} \equiv \langle \psi_{\kappa\mu} \partial_y (\partial^2_{yy} \phi_{\rho\pi} \partial^2_{yz} \psi_{\lambda\nu} - \partial^2_{yz} \phi_{\rho\pi} \partial^2_{yy} \psi_{\lambda\nu}) \rangle,$$

$$I^{(10)}_{\kappa\mu\rho\pi} \equiv \langle \psi_{\kappa\mu} \partial_z (\tfrac{1}{6} z^3 - \tfrac{1}{24} z) \partial^3_{yyy} \phi_{\rho\pi} \rangle.$$

The solution of the system (3.7) of linear inhomogeneous algebraic equations for the coefficients $c_{\lambda\nu}$ is obtained numerically by ordinary matrix inversion techniques. The solution for arbitrary angles $\gamma$ then follows according to relation (3.2).

Once $\psi$ has been determined the modification of the mean shear profile can be computed. The results are shown in figures 2–4. There are two major effects represented in (3.1*d*): the temperature effect and the Reynolds-stress effect, which is dependent on the Prandtl number. Since the basic shear flow $U_0$ originates from the torque caused by the temperature gradient, the modification $U_1$ tends to reduce the shear flow as the growing amplitude of convection establishes a nearly isothermal mean temperature in the interior of the layer. Although thermal boundary layers are formed their torque decreases with an increase in the Nusselt number. The decrease in the stress acting on the boundary is so pronounced that the stress actually decreases with increasing Rayleigh number in the case of air as is evident in figure 2.

The action of the Reynolds stress is more difficult to interpret. As is apparent from figures 3 and 4, the Reynolds stress tends to reverse the shear in the interior of the layer. This is similar to the effect observed by Lipps (1971), who investigated longitudinal convection rolls in the presence of a constant vertical shear applied to the layer. In contrast to his case, not only does the Reynolds stress here decrease the shear in the interior of the layer to zero but an actual reversal originating from the $x$ component of the fluctuating part of the buoyancy force occurs which is not present in the case treated by Lipps.

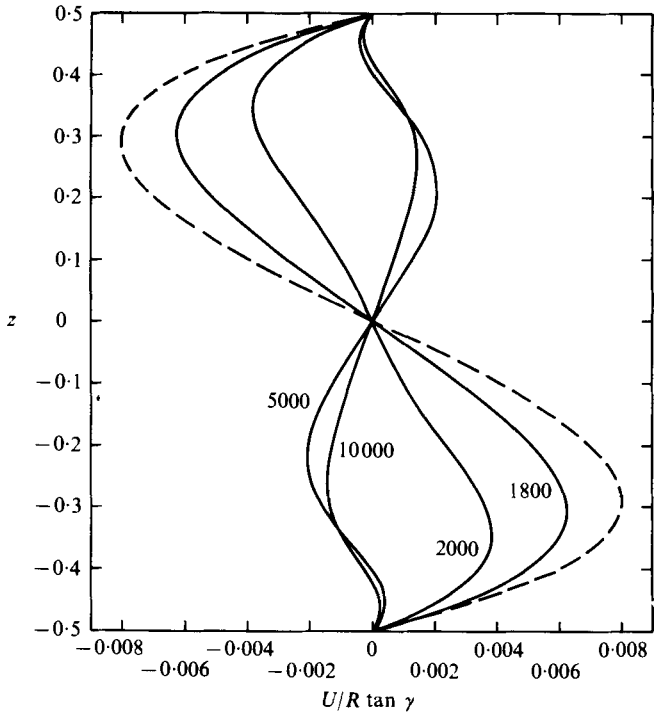


FIGURE 3. The shear-flow velocity profiles $U$ (solid lines) and $U_0$ (dashed line) for an air ($P = 0.71$) layer for various Rayleigh numbers (given on curves).

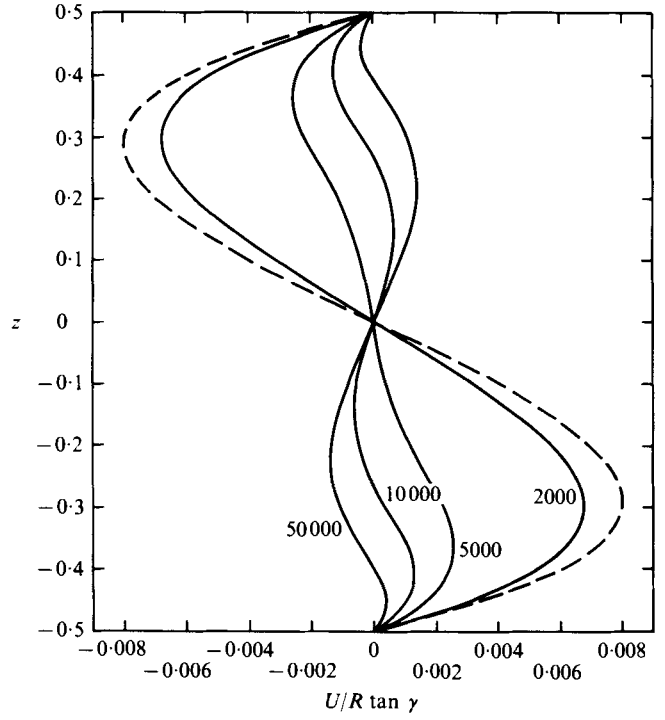


FIGURE 4. The shear-flow velocity profiles $U$ (solid lines) and $U_0$ (dashed line) for a water ($P = 7{\cdot}0$) layer for various Rayleigh numbers (given on curves).

## 4. Stability analysis

In order to investigate the stability of the longitudinal-roll solution we superimpose infinitesimal disturbances. Since the linear system of homogeneous equations for the disturbance variables $\tilde{\phi}$, $\tilde{\theta}$ and $\tilde{\psi}$ does not contain an explicit time dependence we may assume an exponential time dependence $\exp\{\sigma t\}$ for the disturbances. The growth rate $\sigma$ thus becomes the eigenvalue of the linear homogeneous system of equations. If there exists a disturbance for which $\sigma$ has a positive real part the roll solution is unstable. If the eigenvalues of all possible disturbances have vanishing or negative real parts, the roll solution is stable, at least as far as infinitesimal disturbances are concerned.

The equations for the disturbances $\tilde{\phi}$, $\tilde{\psi}$ and $\tilde{\theta}$ are

$$\begin{aligned}\nabla^4\Delta_2\tilde{\phi}+\tan\gamma\partial_{xz}\tilde{\theta}-\Delta_2\tilde{\theta} = {}& P^{-1}\{\boldsymbol{\delta}.[(\boldsymbol{\delta}\tilde{\phi}+\boldsymbol{\epsilon}\tilde{\psi}).\nabla(\boldsymbol{\delta}\phi)]+[(\boldsymbol{\delta}\phi.\nabla)(\boldsymbol{\delta}\tilde{\phi}+\boldsymbol{\epsilon}\tilde{\psi})]\\ &+\partial_t\nabla^2\Delta_2\tilde{\phi}\}+P^{-1}\{\boldsymbol{\delta}.[(\boldsymbol{\delta}\tilde{\phi}+\boldsymbol{\epsilon}\tilde{\psi}).\nabla(\boldsymbol{\epsilon}\psi)\\ &+(\boldsymbol{\epsilon}\psi.\nabla)(\boldsymbol{\delta}\tilde{\phi}+\boldsymbol{\epsilon}\tilde{\psi})]+U\partial_x\nabla^2\Delta_2\tilde{\phi}-(\partial_{zz}U)\partial_x\Delta_2\tilde{\phi}\}, \quad (4.1a)\\ \nabla^2\Delta_2\tilde{\psi}+\tan\gamma\partial_y\tilde{\theta} = {}& P^{-1}\{\boldsymbol{\epsilon}.[(\boldsymbol{\delta}\tilde{\phi}+\boldsymbol{\epsilon}\tilde{\psi}).\nabla(\boldsymbol{\delta}\phi)+(\boldsymbol{\delta}\phi.\nabla)(\boldsymbol{\delta}\tilde{\phi}+\boldsymbol{\epsilon}\tilde{\psi})]\\ &+\partial_t\Delta_2\tilde{\psi}\}+P^{-1}\{\boldsymbol{\epsilon}.[(\boldsymbol{\delta}\tilde{\phi}+\boldsymbol{\epsilon}\tilde{\psi}).\nabla(\boldsymbol{\epsilon}\psi)\\ &+(\boldsymbol{\epsilon}\psi.\nabla)(\boldsymbol{\delta}\tilde{\phi}+\boldsymbol{\epsilon}\tilde{\psi})]+U\partial_x\Delta_2\tilde{\psi}-(\partial_z U)(\partial_y\Delta_2\tilde{\phi})\}, \quad (4.1b)\\ \nabla^2\tilde{\theta}-R\Delta_2\tilde{\phi} = {}& \{(\partial_{yz}\phi-\partial_x\tilde{\psi})\partial_y\theta-(\Delta_2\tilde{\phi})\partial_z\theta\\ &+\partial_{yz}\phi\partial_y\tilde{\theta}-\Delta_2\phi\partial_z\tilde{\theta}+\partial_t\tilde{\theta}\}+\{(\partial_y\psi)\partial_x\tilde{\theta}+U\partial_x\tilde{\theta}\}. \quad (4.1c)\end{aligned}$$

In order to perform a complete stability analysis disturbances of arbitrary three-dimensional spatial dependence must be considered. Since the steady longitudinal-roll solution is periodic in the $y$ direction and does not depend on the $x$ co-ordinate, disturbances of the form

$$\tilde{\phi} = (\sum_{\lambda,\nu}\tilde{a}_{\lambda\nu}e^{i\lambda\alpha y}g_\nu(z))\exp\{i(dy+bx)+\sigma t\}, \quad (4.2a)$$

$$\tilde{\theta} = (\sum_{\lambda,\nu}\tilde{b}_{\lambda\nu}e^{i\lambda\alpha y}f_\nu(z))\exp\{i(dy+bx)+\sigma t\}, \quad (4.2b)$$

$$\tilde{\psi} = (\sum_{\lambda,\nu}\tilde{c}_{\lambda\nu}e^{i\lambda\alpha y}f_\nu(z))\exp\{i(dy+bx)+\sigma t\} \quad (4.2c)$$

can be assumed without loss of generality. Since $\alpha$ is identical to the wavenumber used in the representation of the steady solution given in (3.3) and (3.8), expressions (4.2) exhibit the same periodicity in the $y$ direction as does the roll solution, except for the exponential factor $\exp\{idy\}$. After substituting (4.2) into (4.1) a set of algebraic equations is obtained by using the same procedure as was used in the case of the steady equations:

$$\begin{aligned}&I^{(11)}_{\kappa\mu\lambda\nu}\tilde{a}_{\lambda\nu}+I^{(12)}_{\kappa\mu\lambda\nu}\tilde{b}_{\lambda\nu}+P^{-1}\{I^{(13)}_{\kappa\mu\lambda\nu}\tilde{a}_{\lambda\nu}+I^{(14)}_{\kappa\mu\lambda\nu}\tilde{c}_{\lambda\nu}\}+P^{-1}\{I^{(16)}_{\kappa\mu\lambda\nu}\tilde{a}_{\lambda\nu}+I^{(17)}_{\kappa\mu\lambda\nu}\tilde{c}_{\lambda\nu}\}\\ &\quad+RP^{-1}\tan\gamma I^{(18)}_{\kappa\mu\lambda\nu}\tilde{a}_{\lambda\nu}+\tan\gamma I^{(19)}_{\kappa\mu\lambda\nu}\tilde{b}_{\lambda\nu}=\sigma P^{-1}I^{(15)}_{\kappa\mu\lambda\nu}\tilde{a}_{\lambda\nu}, \quad (4.3a)\\ &I^{(21)}_{\kappa\mu\lambda\nu}\tilde{c}_{\lambda\nu}+P^{-1}\{I^{(22)}_{\kappa\mu\lambda\nu}\tilde{a}_{\lambda\nu}+I^{(23)}_{\kappa\mu\lambda\nu}\tilde{c}_{\lambda\nu}\}+P^{-1}\{I^{(25)}_{\kappa\mu\lambda\nu}\tilde{a}_{\lambda\nu}+I^{(26)}_{\kappa\mu\lambda\nu}\tilde{c}_{\lambda\nu}\}+RP^{-1}\tan\gamma\{I^{(27)}_{\kappa\mu\lambda\nu}\tilde{a}_{\lambda\nu}\\ &\quad+I^{(28)}_{\kappa\mu\lambda\nu}\tilde{c}_{\lambda\nu}\}+\tan\gamma I^{(29)}_{\kappa\mu\lambda\nu}\tilde{b}_{\lambda\nu}=\sigma P^{-1}I^{(24)}_{\kappa\mu\lambda\nu}\tilde{c}_{\lambda\nu}, \quad (4.3b)\\ &I^{(31)}_{\kappa\mu\lambda\nu}\tilde{b}_{\lambda\nu}+RI^{(32)}_{\kappa\mu\lambda\nu}\tilde{a}_{\lambda\nu}+I^{(33)}_{\kappa\mu\lambda\nu}\tilde{a}_{\lambda\nu}+I^{(34)}_{\kappa\mu\lambda\nu}\tilde{c}_{\lambda\nu}+I^{(35)}_{\kappa\mu\lambda\nu}\tilde{b}_{\lambda\nu}\\ &\quad+I^{(37)}_{\kappa\mu\lambda\nu}\tilde{b}_{\lambda\nu}+R\tan\gamma I^{(38)}_{\kappa\mu\lambda\nu}\tilde{b}_{\lambda\nu}=\sigma I^{(36)}_{\kappa\mu\lambda\nu}\tilde{b}_{\lambda\nu}. \quad (4.3c)\end{aligned}$$

The matrices $\mathbf{I}^{(ij)}$ follow from the corresponding terms in (4.1). Since they involve the representation (3.3), (3.8) of the steady roll solution, as well as the representation (4.2) of the disturbances, the expressions for the matrices are lengthy. Because their derivation is straightforward we give only an example:

$$I^{(13)}_{\kappa\mu\lambda\nu} = -\sum_{\rho,\pi} a_{\rho\pi}\langle \mathring{\phi}_{\kappa\mu}\,\boldsymbol{\delta}.\{\boldsymbol{\delta}\mathring{\phi}_{\lambda\nu}.\nabla\boldsymbol{\delta}\phi_{\rho\pi} + \boldsymbol{\delta}\phi_{\rho\pi}.\nabla\boldsymbol{\delta}\mathring{\phi}_{\lambda\nu}\}\rangle.$$

The linear eigenvalue problem (4.3) for the set of unknown coefficients $\tilde{a}_{\lambda\nu}$, $\tilde{b}_{\lambda\nu}$ and $\tilde{c}_{\lambda\nu}$ with $\sigma$ as the eigenvalue is similar to the analogous problem in I governing the stability of the roll solution for a horizontal layer. There are, however, a number of important differences: the number of terms is nearly doubled because of the presence of a component of vorticity normal to the boundaries in the steady solution. As we shall show below, these terms alter the stability properties of the convection rolls. In addition, there are terms associated with the plane parallel shear flow $U$ which by themselves can cause instability. Even though the stability problem given by (4.3) has been solved in the case $\tan\gamma = 0$ and in the case where the amplitude of the roll solution vanishes, these limiting cases are not sufficient to infer the stability properties in the general case. A qualitatively different instability, the wavy instability, occurs at finite angles of inclination and finite amplitudes of convection, as will be discussed in § 5.

For the numerical solution of (4.3) we neglect, as in the case of the steady solution, all equations and coefficients with $|\lambda| + \nu > N$. To ensure convergence of the expansion (4.2), $N$ will be increased until the eigenvalue $\sigma$ does not change significantly when $N$ is replaced by $N+2$. Tests with even higher values of $N$ have shown that this criterion is suitable to ensure a good approximation of the exact solution (see also Denny & Clever 1974). Since interpolation is used to obtain the point at which the maximum of the growth rate $\sigma$ as a function of the wavenumber $b$ is zero additional approximations enter the determination of the critical Rayleigh numbers. Care was taken that the overall uncertainty did not exceed a range of about 2 or 3 %. Following the example of Busse (1967*a*) a considerable simplification of the stability analysis was deduced in I from the symmetry of the stability equations. In the present case one of the symmetry properties is lost, and it is no longer possible to separate the general set (4.2) of disturbances into four subsets. Because of the symmetry of the longitudinal-roll solution it is still possible, however, to separate the disturbances into two subsets corresponding to either a symmetric or an antisymmetric dependence on the $y$ co-ordinate. For simplicity we refer to these two subsets as the symmetric and antisymmetric cases. Hence we rewrite the expansion given in (4.2) (with $d = 0$) as

$$\left.\begin{aligned} \mathring{\phi} &= \sum_{\lambda,\nu} \tilde{a}_{\lambda\nu} g_\nu(z)\, e^{\sigma t} \sin\lambda\alpha y \begin{Bmatrix}\sin bx\\ \cos bx\end{Bmatrix}, \\ \mathring{\psi} &= \sum_{\lambda,\nu} \tilde{c}_{\lambda\nu} f_\nu(z)\, e^{\sigma t} \cos\lambda\alpha y \begin{Bmatrix}\sin bx\\ \cos bx\end{Bmatrix}, \end{aligned}\right\} \quad \textit{antisymmetric case}, \tag{4.4}$$

$$\left.\begin{aligned} \mathring{\phi} &= \sum_{\lambda,\nu} \tilde{a}_{\lambda\nu} g_\nu(z)\, e^{\sigma t} \cos\lambda\alpha y \begin{Bmatrix}\cos bx\\ \sin bx\end{Bmatrix}, \\ \mathring{\psi} &= \sum_{\lambda,\nu} \tilde{c}_{\lambda\nu} f_\nu(z)\, e^{\sigma t} \sin\lambda\alpha y \begin{Bmatrix}\cos bx\\ \sin bx\end{Bmatrix}, \end{aligned}\right\} \quad \textit{symmetric case}, \tag{4.5}$$

where the upper expression in the braces is assumed when $\lambda+\nu$ is odd and the lower expression when $\lambda+\nu$ is even. The expression for $\tilde{\theta}$ is analogous to that for $\tilde{\phi}$ since the two variables have identical symmetry properties. The considerable simplification which has been achieved by replacing (4.2) by (4.4) and (4.5) is expressed by the fact that the summation over $\lambda$ starts at either 0 or 1 instead of at $-\infty$. We note that $\sigma$ is still complex in the otherwise real representations (4.4) and (4.5).

We have introduced the assumption that all physically relevant disturbances correspond to $d = 0$. It was shown in I, in the case $\gamma = 0$, that instabilities with finite values of $d$ are, indeed, of minor importance. Only two types of instability require finite values of $d$: the Eckhaus instability and the hexagonal instability. The Eckhaus instability does not depend on $x$, the co-ordinate parallel to the rolls. Because the $x$-independent equations do not depend on $\tan\gamma$, it will occur in the same way as in the case of a horizontal layer. Since it was shown in I that this instability does not correspond to a transition to a new form of convection as the Rayleigh number increases it has little physical relevance. The hexagonal instability is typical of problems with property variations in the $z$ direction, as discussed by Busse (1967*b*). A recent analysis of this instability in the case of an internally heated layer is given by Clever (1977).

The exclusion of the parameter $d$ is welcome because of the large number of other parameters in the problem. Although it was found that for the majority of the computations at low values of $R-R_c$ a truncation level of $N = 6$ is sufficient to yield reasonably accurate results, the rank of the stability matrix is 51 even at this low truncation level. To test the accuracy and to extend the calculations to higher Rayleigh numbers truncation levels of $N = 8$ and $N = 10$ were used. These correspond to matrices of ranks 92 and 145, respectively.

The principal goal of the stability analysis is to determine the Rayleigh number $R_{\mathrm{II}}$ for the instability of the longitudinal-roll solution as a function of $\gamma$, $P$ and the wavenumber $\alpha$. Even for fixed values of these parameters the determination of $R_{\mathrm{II}}$ involves a considerable amount of computation since the eigenvalue $\sigma$ with largest real part must be determined as a function of the disturbance wavenumber $b$. After this eigenvalue has been calculated for several Rayleigh numbers, selected in such a way that the eigenvalue with largest real part crosses zero, the value of $R_{\mathrm{II}}$ is then accurately determined by interpolation. Fortunately, the value of $R_{\mathrm{II}}$ for the wavy instability is found to be rather insensitive to variations in $b$ in the case of moderate angles $\gamma$ ($\gamma \lesssim 70°$) since the critical disturbance corresponds to vanishing $b$. Hence it was possible to get accurate results by choosing a small value of $b$, say $b = 0{\cdot}1$, which was actually used for the majority of the computations. In representative cases the growth rate $\sigma$ was calculated as a function of $b$ for supercritical as well as subcritical Rayleigh numbers.

Most of the calculations were done for $\alpha = \alpha_c \equiv 3{\cdot}117$, which is the critical value at the onset of longitudinal rolls. However, different values of $\alpha$ are often realized experimentally and the mechanism of instability depends on this parameter. For this reason the dependence of $R_{\mathrm{II}}$ on $\alpha$ has been investigated for some particular cases. The dependence on the parameter $P$ is not extensively represented in the results because of the limitations imposed by the costs of computations. Two Prandtl numbers, $P = 0{\cdot}71$ and $P = 7{\cdot}0$, corresponding to air and water respectively, were selected as representative for the dependence of the wavy instability (see § 5) on the Prandtl number and for comparison with experimental results. For low Prandtl numbers

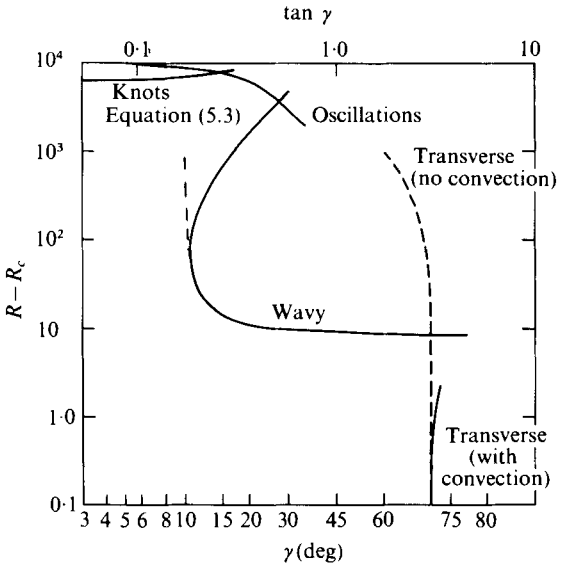


FIGURE 5. The various instabilities for an inclined air ($P = 0{\cdot}71$) layer. For $R$ greater than the values given by the curves (except for the transverse instabilities) longitudinal convection rolls undergo transition. In the case of the transverse instabilities, for $\gamma$ greater than the values given by the curves instability occurs.

($P \lesssim 0{\cdot}22/\cos\gamma$ for $\gamma \lesssim 89°$) a steady transverse instability precludes the onset of longitudinal rolls (except for small $\gamma$) whereas for high Prandtl numbers the wavy instability occurs only at large Rayleigh numbers, if it occurs at all, for which the computational costs are prohibitive. The two Prandtl numbers selected illustrate the wavy instability between these two limits. The dependence of the Rayleigh number $R_{\mathrm{II}}$ on the angle $\gamma$ has received special attention, since the layer inclination can be most easily varied in experiments. Most of the results will be shown as a function of the angle $\gamma$, and the discussion of the instability mechanism will focus on this parameter.

## 5. The wavy instability

The fact that longitudinal rolls represent a secondary solution of the equations for an inclined layer heated from below is expressed by the periodic dependence in the $y$ direction, which is not reflected in the physical conditions of the problem. For this reason an arbitrary translation in the $y$ direction produces a solution with the same physical properties as the original solution. A consequence of this translational invariance is the fact that

$$(\tilde{\phi}, \tilde{\psi}, \tilde{\theta}) = (\partial_y \phi, \partial_y \psi, \partial_y \theta) \tag{5.1}$$

represents a solution of the stability equations (4.1) corresponding to $\sigma = 0$. We note that as in (4.1) the scalar functions $\phi$, $\psi$ and $\theta$ refer to the longitudinal-roll solution. The eigenvalue $\sigma = 0$ does not indicate instability. It is possible, however, that small additional physical effects may lead to a positive real part of $\sigma$. This is in fact the basic origin of the wavy instability, at least in the parameter range where it occurs for small values of $b$.

Instability related to the property (5.1) has been discussed in the case of convection in a horizontal layer. It was shown theoretically by Busse (1967*a*, *b*) and experimentally

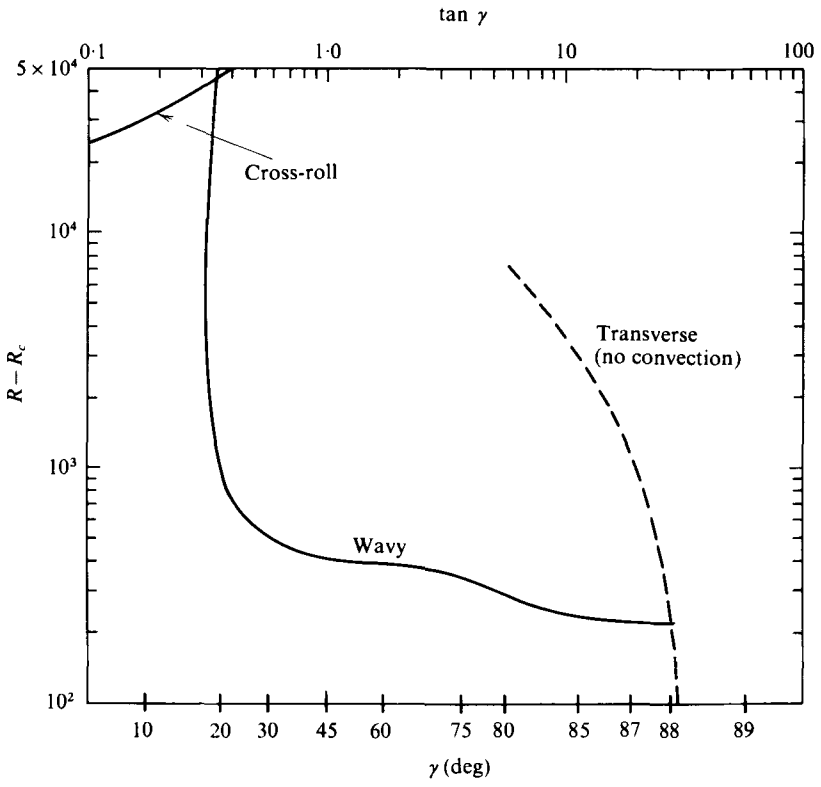


FIGURE 6. The various instabilities for an inclined water ($P = 7{\cdot}0$) layer. For $R$ greater than the values given by the curves (except for the transverse instability) longitudinal convection rolls are unstable. The dashed curve shows the stability boundary for transverse modes (without longitudinal convection rolls).

by Busse & Whitehead (1971) that an instability of the form (5.1) with an additional dependence exp $\{ibx\}$ for small values of $b$ occurs when the value $\alpha$ of the roll wavenumber is sufficiently less than the critical value $\alpha_c$. In the inclined convection layer an instability of the same kind may occur for all wavenumbers $\alpha$ of the steady solution. Hence the instability produces a transition to a different form of convection in this case. In this paper we call this the wavy instability because of the characteristic wavy (although non-oscillatory) form of the resulting convection pattern. In the paper by Busse & Whitehead (1971) the instability was called the zigzag instability because it produced convection rolls in a typical herring-bone pattern.

In accordance with the above description, the wavy instability is obtained in the case of antisymmetric disturbances (4.4). The Rayleigh number $R_{\text{II}}$ for onset of this instability is plotted in figures 5 and 6 as a function of tan $\gamma$ for the two different Prandtl numbers. Since the transition does not occur in the horizontal case, $R_{\text{II}}$ tends to infinity at a finite value of $\gamma$ which depends on the Prandtl number. A qualitative understanding of the dependence of $R_{\text{II}}$ can be obtained from a small amplitude expansion of the problem analogous to that used by Schlüter, Lortz & Busse (1965) and Busse (1967*b*). Using both the amplitude $\epsilon$ of longitudinal-roll convection and tan $\gamma$ as perturbation parameters we find

$$\sigma = -b^2\{\tan^2\gamma(A - \epsilon^2 B) + \epsilon^2 C + \ldots\}, \tag{5.2}$$

where terms of higher order in $\tan\gamma$ and $\epsilon$ have been neglected. In addition we have used the fact $\sigma$ is proportional to $b^2$ for non-oscillatory disturbances which reduce to (5.1) in the limit of vanishing $b$. Without proof we note that the symmetry of the problem requires that only even powers of both $\tan\gamma$ and $\epsilon$ enter relation (5.2). The constant $A$ must be positive since all $x$-dependent disturbances [excluding symmetric disturbances (4.4)] of the inclined layer decay at the Rayleigh number $R = R_c$ for the onset of longitudinal rolls. In addition it is known that the instability does not occur in the case of a horizontal layer. Hence $C$ must be positive. The fact that the wavy instability occurs in an inclined layer suggests that $B$ assumes a positive value. Using the approximate relation

$$R = R_c + \epsilon^2 R^{(2)} + \ldots$$

for the Rayleigh number as a function of the amplitude $\epsilon$ of the longitudinal rolls we obtain the expression

$$R_{\mathrm{II}} - R_c = \frac{\tan^2\gamma A/R^{(2)}}{B\tan^2\gamma - C} \tag{5.3}$$

by setting $\sigma$ equal to zero. The constants $A$, $B$ and $C$ can be calculated by using either independent programs or the present program in the limit when $\tan\gamma$ and $\epsilon$ tend to zero. In the case of air we find, using the latter approach,

$$A/CR^{(2)} = 322{\cdot}8, \quad B/C = 36{\cdot}89. \tag{5.4}$$

The approximate relationship (5.3) is shown in figure 5 for comparison with the numerical results. The simple model appears to describe the transition rather well and emphasizes the point that the transition does not exist for angles less than a critical value $\gamma_c$, which in the approximate formulation is given by

$$\gamma_c = \arctan\,(C/B)^{\frac{1}{2}}. \tag{5.5}$$

Because the transition occurs for much higher Rayleigh numbers in the case of water the quantitative agreement with the approximate expression (5.3) is not as good as in the case of air. It is evident from figure 6, however, that the qualitative dependence of $R_{\mathrm{II}}$ is the same.

For large values of $\tan\gamma$ the wavy instability changes character. The change is most clearly evident in figure 6, where a point of inflexion in the stability boundary occurs for $\gamma \approx 65°$. While for lower angles the wavy instability is governed by the translational mechanism discussed above, the basic shear flow becomes sufficiently strong for larger angles to dominate the mechanism of instability.

The change in character of the wavy instability at $\gamma \approx 65°$ is associated with a change in the wavenumber $b$ of the critical disturbance. We have mentioned earlier that for moderate angles of inclination the instability always reaches a positive growth rate $\sigma$ first in the limit of small wavenumbers $b$. For large angles $\gamma$ this behaviour is changed, as is demonstrated in figure 7. The typical value $b$ of the most unstable wave is of order unity in this case. The fact that a finite value of $b$ is observed experimentally also for low values of $\gamma$ does not contradict the theoretical result. Since the growth rate reaches a maximum at a finite value of $b$ as soon as the critical Rayleigh number is exceeded by a small amount it becomes difficult to determine the critical value of the wavenumber $b$.

For large $\gamma$ we have not performed detailed computations of the function $R_{\mathrm{II}}$ since

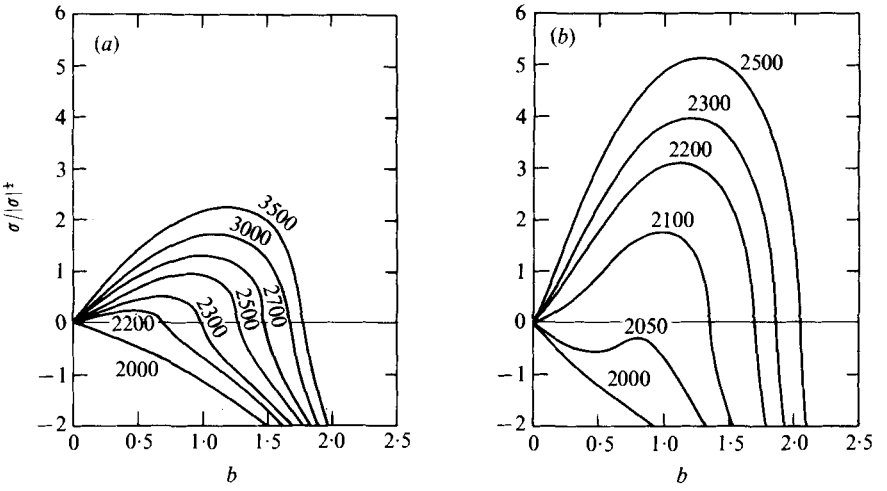


FIGURE 7. The dependence on the $b$ wavenumber of the growth rate for a water ($P = 7{\cdot}0$) layer at (*a*) $\gamma = 45°$ and (*b*) $\gamma = 75°$, showing the change in character of the instability at large $\gamma$. The wavy instability *first* emerges as a disturbance with (*a*) a vanishing or (*b*) a finite value of the $b$ wavenumber. The numbers on the curves give the Rayleigh numbers.

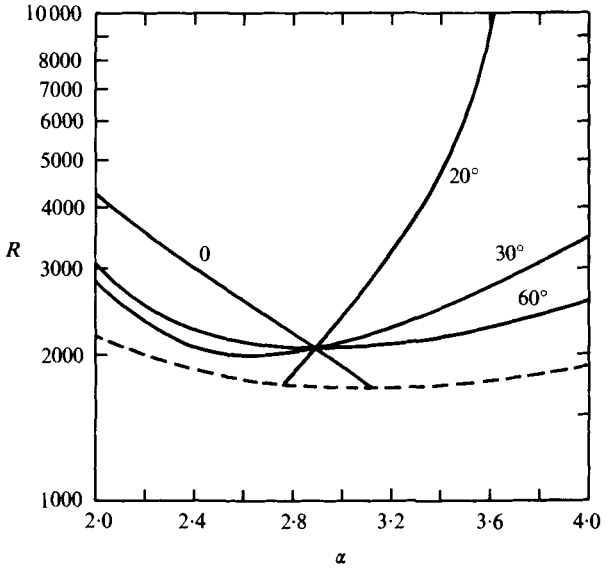


FIGURE 8. The dependence of $R_{II}$ on the $\alpha$ wavenumber at various angles $\gamma$ (given on curves) for a water layer ($P = 7{\cdot}0$). For $R$ less than the values given on the curves (except $\gamma = 0$) two-dimensional longitudinal convection rolls are *stable*. For $\gamma = 0$, two-dimensional rolls are *unstable* for $R$ less than the values given by the curve. – – –, $R_c$ onset of convection rolls.

the longitudinal rolls are unstable for Rayleigh numbers less than $R_{II}$ owing to the transverse instability. This instability, which will be discussed in § 7, represents an optimally adjusted mode among all modes generated by the shear instability mechanism.

To demonstrate the dependence of $R_{II}$ on the wavenumber $\alpha$ of the longitudinal rolls detailed calculations have been performed for the case of water. The results

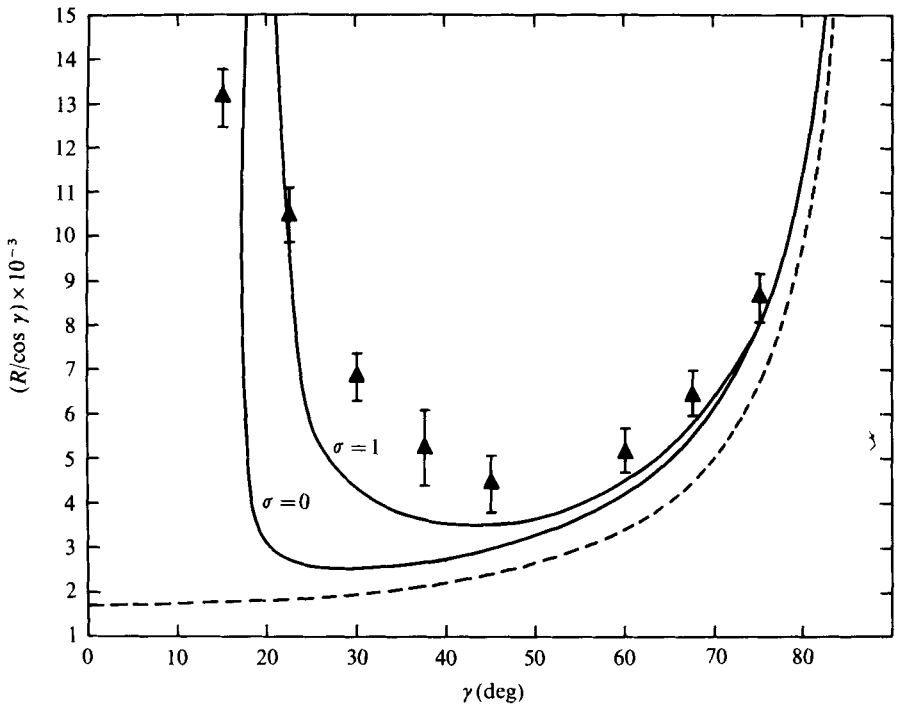


FIGURE 9. $R_{\mathrm{II}}$ plotted as a function of the angle of inclination using Hart's Rayleigh number $R^* = R/\cos\gamma$. To show where large discrepancies between experimental observations and theoretical predictions must be expected the curve $\sigma = 1$ for the most strongly growing disturbance is shown for comparison ⊥, $R_{\mathrm{II}}$, experiment (Hart); ——, $R_{\mathrm{II}}$, theory; – – –, $R_c$ onset of convection rolls.

shown in figure 8 clearly demonstrate the connexion between the wavy instability and the zigzag instability which occurs in a horizontal layer. For $\gamma = 0$ the zigzag instability limits the stability range of rolls towards small $\alpha$. The transition from stable rolls to zigzagging rolls occurs with decreasing Rayleigh number at a given value of $\alpha$. At the critical angle $\gamma_c \approx 17°$ the stability boundary 'tips over' and a transition with increasing Rayleigh number becomes possible. For larger angles the wavy instability depends little on the wavenumber $\alpha$. As the shear-flow mechanism of instability becomes dominant, the dependence on $\alpha$ is expected to vanish.

The most detailed experimental observations of the onset of the wavy instability have been made by Hart (1971*a*, *b*). The photographs in his paper clearly demonstrate the bending of the rolls as the instability sets in. Because of the finite aspect ratio of the experimental apparatus and the difficulty in observing small disturbances, close quantitative agreement between observations and theory cannot be expected. Figure 9, however, does indicate reasonable correspondence. This figure has been drawn in terms of the Rayleigh number $R^* = R/\cos\gamma$, which is preferred by experimentalists, since the definition is the same as in the case of a horizontal layer. To emphasize the difficulty of determining the onset of instability in an experiment with slowly increasing Rayleigh number we have drawn the curve for $\sigma = 1$ in addition to the curve $\sigma = 0$ of marginal stability. Since only disturbances growing at a finite rate are observed experimentally it is not surprising that the experimental observations of

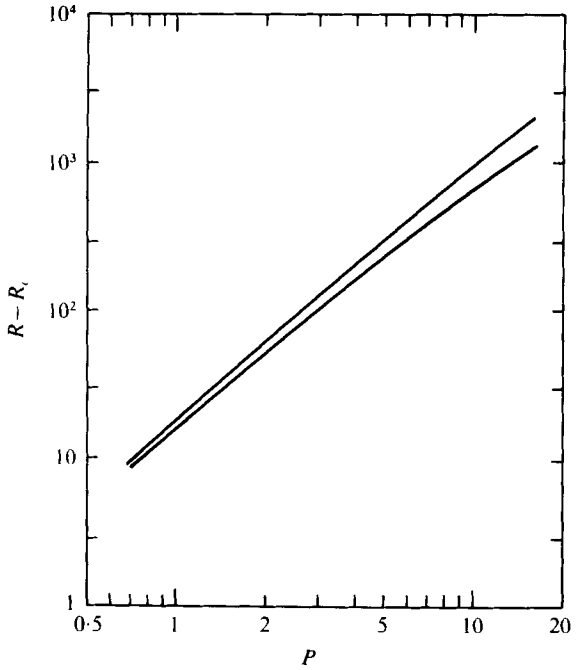


FIGURE 10. The Prandtl number dependence of the wavy instability. The lower and upper curves are for $\gamma = 60°$ and 30°, respectively.

the onset of instability deviate from the theoretical predictions wherever the growth rate of the disturbance is relatively low. Since the growth rate of disturbances increases relatively slowly with $R - R_{II}$ at angles between 20° and about 45° according to figure 9, discrepancies between the observed onset of instability and the theoretical neutral curve must be expected in that region. Indeed, since the Rayleigh number in Hart's (1971*b*) experiment increases by about 1500 within a thermal time scale and since disturbances usually require a growth time of 2 or 3 time units to become visible, the observational data are in reasonable agreement with the theoretical predictions if the growth-rate effect is taken into account. Hart's observations of the wavelength of the wavy rolls are consistent with this interpretation and the theoretical values for the $b$ wavenumber of the most strongly growing disturbance, since this $b$ wavenumber increases significantly at slightly supercritical Rayleigh numbers according to figures 7 (*a*) and (*b*).

Hart (1971*b*) suggested an interpretation of his experimental observations in terms of an instability mechanism based on the buoyancy component parallel to the layer. While his estimates seem to indicate reasonable agreement with experimental observations in the case of water, large discrepancies must be expected for other Prandtl numbers. In contrast to Hart's Prandtl-number-independent mechanism, the rigorous theoretical results clearly demonstrate a strong Prandtl-number dependence of $R_{II}$, which indicates that the instability originates from the momentum-advection terms of the equation of motion. To establish this point additional calculations have been done for the case $P = 16$ for two angles of inclination. The results shown in figure 10 indicate a nearly quadratic growth of $R_{II}$ with Prandtl number, which is the expected dependence for the action of the momentum-advection terms.

## 6. The oscillatory instability

In contrast to the wavy instability the oscillatory instability causes a transition (for $\alpha = 3{\cdot}117$) in the case of a horizontal layer. At the transition Rayleigh number $R_{\mathrm{III}}$, convection in the form of steady rolls is transformed into oscillatory rolls, at least in the case of Prandtl numbers of the order of 5 or less. As was emphasized in the first theory of this transition by Busse (1972), the growing oscillatory disturbances can be understood as slight modifications of the translational disturbance (5.1) similar to the wavy instability. In contrast to the latter, a mean component of vertical vorticity is associated with the oscillatory disturbances in the horizontal layer. In the case of the inclined layer this distinction is less pronounced since the basic longitudinal-roll solution is already associated with a component of normal vorticity, which increases in proportion to $\tan\gamma$ according to relation (3.2). The disturbances still show a considerable difference in the coefficient $\tilde{c}_{01}$ of $\tilde{\psi}$, however, depending on whether or not the imaginary part of $\sigma$ vanishes.

It is not always easy to distinguish experimentally the oscillatory from the wavy instability and observations are sometimes ambiguous since the imaginary part of $\sigma$ may be rather small. Since both instabilities belong to the class of antisymmetric disturbances, they are mainly distinguished theoretically by the fact that the eigenvalue $\sigma$ is complex in the case of the oscillatory instability.

The Rayleigh number $R_{\mathrm{III}} - R_c$ for the onset of oscillations is roughly proportional to the square of the Prandtl number. The same fact holds approximately for $R_{\mathrm{II}} - R_c$, which indicates that both instabilities are caused by the momentum-advection terms in the equation of motion. As shown in figure 5, $R_{\mathrm{III}}$ decays as $\tan\gamma$ increases. Thus the oscillatory instability parallels the behaviour of the wavy instability with the exception of the dependence on the wavenumber $b$. The real part of the growth rate always reaches positive values at a finite value of $b$, as was shown in I in the case of the horizontal layer.

Since $R_{\mathrm{III}}$ exceeds $R_{\mathrm{II}}$ for most values of $\gamma$ the oscillatory instability is physically realized only for either very small angles of inclination or possibly for values of the Prandtl number greater than about 10 (Korpela, Gözüm & Chandakant 1973). The experimental observations by Hart (1971*a*) indicate, however, that the wavy rolls become oscillatory, i.e. travelling waves, at Rayleigh numbers not far from $R_{\mathrm{III}}$. Thus the stability analysis for oscillatory disturbances appears to be physically relevant even though it is not applicable in a rigorous sense for Rayleigh numbers exceeding $R_{\mathrm{II}}$.

The dependence of $R_{\mathrm{III}}$ on the wavenumber $\alpha$ of the longitudinal rolls has not been calculated. The $\alpha$ dependence has been calculated in I for a horizontal convection layer with $P = 0{\cdot}71$. Since the oscillatory instability normally occurs at this Prandtl number only for $\gamma \leqslant 10^\circ$ it can be expected that the $\alpha$ dependence is similar to the case $\gamma = 0$.

## 7. The transverse instability

Both the wavy and the oscillatory instability belong to the antisymmetric class of disturbances (4.4). Symmetric instabilities of the form (4.5) appear to be of lesser importance for convection in an inclined layer for angles at which the heating is from

below. In the case of the horizontal layer examples of symmetric instabilities are the cross-roll instability and the knot instability, which lead to bimodal convection and spoke rolls, respectively, at Rayleigh numbers of the order of $2 \times 10^4$ and higher. The transition to bimodal convection has been discussed in I. The knot instability differs essentially only by its smaller $b$ wavenumber and is discussed in detail in a forthcoming paper (Busse & Clever 1977). The latter instability limits the stability region of rolls for Prandtl numbers $P$ in the range $1 \lesssim P \lesssim 10$ and is therefore of particular interest in the present analysis. Both instabilities tend to introduce rolls at right angles to the given longitudinal rolls and thus become inhibited by the shear flow as the angle increases as is shown in figure 6. The stabilizing effect of the shear is particularly well demonstrated in the high Prandtl number experiments by Richter & Whitehead (1974) and Richter & Parsons (1975), in which the shear was introduced through relative motion of the upper boundary. Stable longitudinal rolls are found in these experiments for $R = 5 \times 10^5$ at a Prandtl number of $10^4$.

Besides its stabilizing effect, the shear flow also provides a destabilizing action. The cubic shear-flow profile is characterized by an inflexion point and is therefore subject to instability according to Rayleigh's criterion. Squire's (1933) theorem states that in the absence of temperature gradients the instability first appears in the form of transverse disturbances which are independent of the $y$ co-ordinate. In the case of the inclined layer heated from below Gershuni & Zhukovitskii (1969) have shown by an extension of Squire's theorem that the instability of the basic state occurs in the form of $y$-independent disturbances unless convection in the form of $x$-independent longitudinal rolls sets in at a lower Rayleigh number.

The goal of our analysis in this connexion is to investigate the modification of the transverse instability when longitudinal convection rolls are present. Obviously the transverse disturbances belong to the symmetric case (4.5) since the function $\tilde{\phi}$ must include the $y$-independent component. From the analysis of Gershuni & Zhukovitskii (1969) it is evident, however, that nearly transverse disturbances show positive growth rates at Rayleigh numbers only slightly above that for the onset of the transverse instability. Nearly transverse disturbances can be described, however, both by the symmetric and by the antisymmetric case. Indeed, in discussing the wavy instability and the oscillatory instability we have already pointed out that the influence of the shear mechanism of instability becomes increasingly pronounced for large angles of inclination. Since growth rates of nearly transverse symmetric disturbances are close to the growth rate of the transverse instability the numerical computations show unsatisfactory convergence unless the truncation parameter $N$ is increased to a rather high level. In figures 2 and 3 the onset of the transverse instability in the absence of longitudinal rolls is shown by a dashed line. The presence of convection rolls has a stabilizing influence, as shown by the solid line in figure 5. This line was obtained using $N = 15$ as the truncation parameter, with a modification of the truncation scheme whereby modes with $3|\lambda| + \nu > N$ were neglected in the computations. The lack of convergence and the prohibitive expense of computations at higher values of $N$ have prevented us from extending the solid line to higher Rayleigh numbers.

In the range of the Prandtl numbers including those of air and water the transverse instability sets in as a monotonically growing disturbance. Hence our calculations have exhibited eigenvalues with a vanishing imaginary part. It should be mentioned, however, that at higher Prandtl numbers, of the order of 10 and larger, as $\gamma \to \frac{1}{2}\pi$ an

oscillatory transverse instability sets in before the onset of the steady transverse instability. The corresponding analysis in the case without convection is given by Gershuni & Zhukovitskii (1969) and Korpela *et al.* (1973).

## 8. Concluding remarks

The transition from longitudinal to wavy convection rolls is a common feature of many cases of roll-like motions in the presence of mean shear. The various forms of wavy Taylor vortices are probably the best known examples (Coles 1965; Snyder 1970). Observations by Bénard & Avsec (1938) of convection in the presence of plane Couette flow show wavy rolls similar to those observed by Hart (1971*a*, *b*) in the inclined convection layer. There can be little doubt that the basic mechanism of instability is essentially the same even though the experimental contexts differ widely. The translational invariance of the longitudinal convection rolls and the presence of a component of vorticity normal to the boundary give rise to the wavy instability (or to the oscillatory instability, depending on the parameter range) when the Reynolds number of the mean shear is sufficiently small. The instability is modified and characterized by a higher value of the longitudinal wavenumber $b$ when the Reynolds number of the mean shear becomes comparable to that for which transverse instability would occur in the absence of the roll component of motion. In this region the usual transverse instability competes with the wavy instability. Unfortunately Hart's (1971*a*, *b*) experiments do not extend to high enough angles of inclination to give an experimental determination of the angle of transition between the two types of instability.

In the case of the Taylor vortex the onset of the various instabilities is modified by the effects of the Coriolis force and the curvature. The theoretical analysis by Davey, DiPrima & Stuart (1968) is restricted to small amplitudes of the Taylor vortex and does not consider all possible disturbances. The mechanism for the wavy instability, however, is similar to that considered in this paper. An extension of the analysis of Davey *et al.* (1968) along the lines of the present work is planned in order to resolve the remaining discrepancies between theory and experiment pointed out by Snyder (1970).

The research reported in this paper was supported by the U.S. Army Research Office, Durham, and by the National Science Foundation under Grant DES 71-00543. A major portion of the numerical analysis was made possible through funds supplied by the Campus Computing Network at UCLA. The authors wish to thank Professor Robert E. Kelly for his assistance and helpful suggestions throughout all phases of this investigation.

REFERENCES

BÉNARD, H. & AVSEC, D. 1938 Travaux récents sur les tourbillons cellulaires et les tourbillons en bandes. Applications a l'astrophysique et la météorologie. *J. Phys. Radium* **9**, 486–500.

BUSSE, F. H. 1967*a* On the stability of two-dimensional convection in a layer heated from below. *J. Math. & Phys.* **46**, 140–150.

BUSSE, F. H. 1967*b* The stability of finite amplitude cellular convection and its relation to an extremum principle. *J. Fluid Mech.* **30**, 625–649.

BUSSE, F. H. 1971 In *Instability of Continuous Systems* (ed. H. Leipholz), pp. 41–47. Springer.

BUSSE, F. H. 1972 The oscillatory instability of convection rolls in a low Prandtl number fluid. *J. Fluid Mech.* **52**, 97–112.

BUSSE, F. H. & CLEVER, R. M. 1977 The knot instability of convection rolls in fluids of moderate Prandtl numbers. (In preparation.)

BUSSE, F. H. & WHITEHEAD, J. A. 1971 Instabilities of convection rolls in a high Prandtl number fluid. *J. Fluid Mech.* **47**, 305–320.

CHANDRASEKHAR, S. 1961 *Hydrodynamic and Hydromagnetic Stability.* Oxford : Clarendon Press.

CLEVER, R. M. 1973 Finite amplitude longitudinal convection rolls in an inclined layer. *J. Heat Transfer* **95**, 407–408.

CLEVER, R. M. 1977 The stability and heat transfer of two-dimensional convection in an internally heated fluid layer. *Z. angew. Math. Phys.* (in press).

CLEVER, R. M. & BUSSE, F. H. 1974 Transition to time-dependent convection. *J. Fluid Mech.* **65**, 625–645.

COLES, D. 1965 Transition in circular Couette flow. *J. Fluid Mech.* **21**, 385–425.

DAVEY, A., DIPRIMA, R. C. & STUART, J. T. 1968 On the stability of Taylor vortices. *J. Fluid Mech.* **31**, 17–52.

DENNY, V. E. & CLEVER, R. M. 1974 Comparisons of Galerkin and finite difference methods for solving highly nonlinear thermally driven flows. *J. Comp. Phys.* **16**, 271–284.

GERSHUNI, G. Z. & ZHUKOVITSKII, E. M. 1969 Stability of plane parallel convective motion with respect to spatial perturbations. *Prikl. Math. Mech.* **33**, 830–835.

HART, J. E. 1971*a* The stability of flow in a differentially heated inclined box. *J. Fluid Mech.* **47**, 547–576.

HART, J. E. 1971*b* Transition to a wavy vortex regime in convective flow between inclined plates. *J. Fluid Mech.* **48**, 265–271.

HART, J. E. 1973 A note on the structure of thermal convection in a slightly slanted slot. *Int. J. Heat Mass Transfer* **16**, 747–753.

KORPELA, S. A., GÖZÜM, D. & CHANDAKANT, B. B. 1973 On the stability of the conduction regime of natural convection in a vertical slot. *Int. J. Heat Mass Transfer* **16**, 1683–1690.

KRISHNAMURTI, R. 1970*a* On the transition to turbulent convection. Part 1. The transition from two- to three-dimensional flow. *J. Fluid Mech.* **42**, 295–307.

KRISHNAMURTI, R. 1970*b* On the transition to turbulent convection. Part 2. The transition to time-dependent flow. *J. Fluid Mech.* **42**, 309–320.

KRISHNAMURTI, R. 1974 Some further studies on the transition to turbulent convection. *J. Fluid Mech.* **60**, 285–303.

LIPPS, F. B. 1971 Two-dimensional numerical experiments in thermal convection with vertical shear. *J. Atmos. Sci.* **28**, 3–19.

RICHTER, F. & PARSONS, B. 1975 On the interaction of two scales of convection in the mantle. *J. Geophys. Res.* **80**, 2529–2541.

RICHTER, F. & WHITEHEAD, J. A. 1974 Rayleigh–Bénard convection at large Prandtl numbers with shear. *Bull. Am. Phys. Soc.* **19**, 1159.

SCHLÜTER, A., LORTZ, D. & BUSSE, F. H. 1965 On the stability of steady finite amplitude convection. *J. Fluid Mech.* **23**, 129–144.

SNYDER, A. A. 1970 Waveforms in rotating Couette flow. *Int. J. Non-Linear Mech.* **5**, 659–685.

SPARROW, E. M. & HUSAR, R. B. 1969 Longitudinal vortices in natural convection flow on inclined plates. *J. Fluid Mech.* **37**, 251–255.

SQUIRE, H. B. 1933 On the stability for three-dimensional disturbances of viscous fluid flow between parallel walls. *Proc. Roy. Soc.* **142**, 621–628.

WILLIS, G. E. & DEARDORFF, J. W. 1970 The oscillatory motions of Rayleigh convection. *J. Fluid Mech.* **44**, 661–672.